



A correction to the analysis of bending under tension tests

Nielsen, C.V.; Legarth, B.N.; Niordson, C.F.; Bay, N.

Published in:
Tribology International

Link to article, DOI:
[10.1016/j.triboint.2022.107625](https://doi.org/10.1016/j.triboint.2022.107625)

Publication date:
2022

Document Version
Publisher's PDF, also known as Version of record

[Link back to DTU Orbit](#)

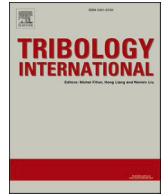
Citation (APA):
Nielsen, C. V., Legarth, B. N., Niordson, C. F., & Bay, N. (2022). A correction to the analysis of bending under tension tests. *Tribology International*, 173, Article 107625. <https://doi.org/10.1016/j.triboint.2022.107625>

General rights

Copyright and moral rights for the publications made accessible in the public portal are retained by the authors and/or other copyright owners and it is a condition of accessing publications that users recognise and abide by the legal requirements associated with these rights.

- Users may download and print one copy of any publication from the public portal for the purpose of private study or research.
- You may not further distribute the material or use it for any profit-making activity or commercial gain
- You may freely distribute the URL identifying the publication in the public portal

If you believe that this document breaches copyright please contact us providing details, and we will remove access to the work immediately and investigate your claim.



A correction to the analysis of bending under tension tests

C.V. Nielsen^{*}, B.N. Legarth, C.F. Niordson, N. Bay

Department of Civil and Mechanical Engineering, Technical University of Denmark, 2800 Kgs., Lyngby, Denmark

ARTICLE INFO

Keywords:
Friction
Simulative test
Bending under tension

ABSTRACT

The existing analytical solutions for determining an average coefficient of friction in bending under tension tests are revisited. The most commonly used equations are based on the assumption of uniform pressure in the contact interface, which is proven to be a statically inadmissible assumption. New analytical solutions are presented based on the assumption of concentrated forces, which are shown to be statically admissible. Existing literature supports the existence of localized peaks in the pressure distribution in terms of both numerical simulations and experimental results. Due to the inhomogeneous pressure distribution, bending under tension tests are not considered appropriate for determining the coefficient of friction, but rather a qualitative test capable of relative comparison of tribo-systems.

1. Introduction

The deformation and contact conditions over the die curvature in deep drawing, Fig. 1a, are often analyzed by the simplified simulative test shown in Fig. 1b. The simulative test is a plane bending under tension test, which was first reported by Swift [1] in analysis of plasticity and later by Littlewood and Wallace [2] in analysis of friction and wear. A flat workpiece is drawn over a 90° die radius by the drawing force F_1 while an opposing force F_2 gives rise to back tension, which in the deep drawing case would stem from the restricted flow along corners and restraining forces imposed by the blank holder and draw beads. Wilson et al. [3] developed the sheet metal forming simulator schematically shown in Fig. 1c. The principle is the same as that of Fig. 1b, but the contact angle θ can be varied and the pin tool is mounted on a shaft that can be rotated by an electromotor or kept stationary to vary the relative sliding velocity between strip and tool.

2. Existing analytical calculations of the friction coefficient

2.1. The belt/pulley/capstan formula

Assuming the strip fully flexible like a belt, requiring no force to bend and unbend over the die radius, the belt/pulley/capstan formula (Highdon and Stiles [4]) can be applied to calculate the coefficient of friction μ . The orientation of Fig. 1c will be adopted in the analytical analyses. With reference to Fig. 2, radial force equilibrium gives

$$pRwd\varphi = (2F + dF)\sin\frac{d\varphi}{2} \cong 2F\frac{d\varphi}{2} \quad (1)$$

$$\Leftrightarrow p = \frac{F}{Rw} \quad (2)$$

where p is the normal pressure and w is the strip width. Moment equilibrium around the center of the circular arc results in

$$dFR = \mu p w R^2 d\varphi \quad (3)$$

Inserting (2) into (3) and solving the differential equation with the boundary conditions being the forces F_1 and F_2 at the outlet and inlet, respectively, of the contact zone spanning the angle θ yields the following expression for the friction coefficient μ :

$$\frac{dF}{F} = \mu d\varphi \quad (4)$$

$$\Leftrightarrow \mu = \frac{1}{\theta} \ln \frac{F_1}{F_2} \quad (5)$$

In the special case of a 90° bend, the friction coefficient becomes

$$\mu = \frac{2}{\pi} \ln \frac{F_1}{F_2} \quad (6)$$

Swift [1] analyzed the stress-strain states of plastic bending under tension and presented an apparatus where he could bend the strip over a tool pin, which could be allowed to rotate or remain stationary. He could thereby separate effects from friction and bending. Doege and Witthüser [5] applied this strategy to remove the influence of bending and

^{*} Corresponding author.

E-mail address: cvni@mek.dtu.dk (C.V. Nielsen).

Nomenclature	
F	Axial force
F_1	Drawing force
F_2	Back tension force
F_b	Bending and unbending force
p	Normal pressure
Q_1	Concentrated force at outlet
Q_2	Concentrated force at inlet
R	Tool radius
t	Strip thickness
T	Torque
w	Strip width
θ	Contact angle
μ	Coefficient of friction
μ_{90}	Coefficient of friction at 90° contact angle
τ	Friction stress
φ	Angular position

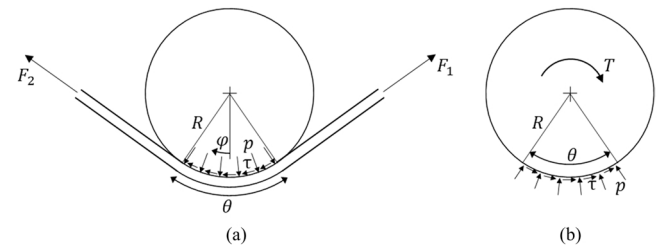


Fig. 3. Bending under tension analyzed under the assumption of uniformly distributed normal pressure p and friction stress τ over the contact spanned by the angle θ . (a) Shows the loads on the strip and (b) shows the loads from the strip to the tool and the necessary torque T for moment equilibrium.

expression for the average coefficient of friction by taking the ratio between strip thickness t and tool pin radius R into account. Following (1)-(6) with R replaced by $R + \frac{t}{2}$ in the left hand side of (3) result in their expression,

$$\mu_{90} = \frac{2}{\pi} \left(\frac{2R+t}{2R} \right) \ln \left(\frac{F_1 - F_b}{F_2} \right) \quad (8)$$

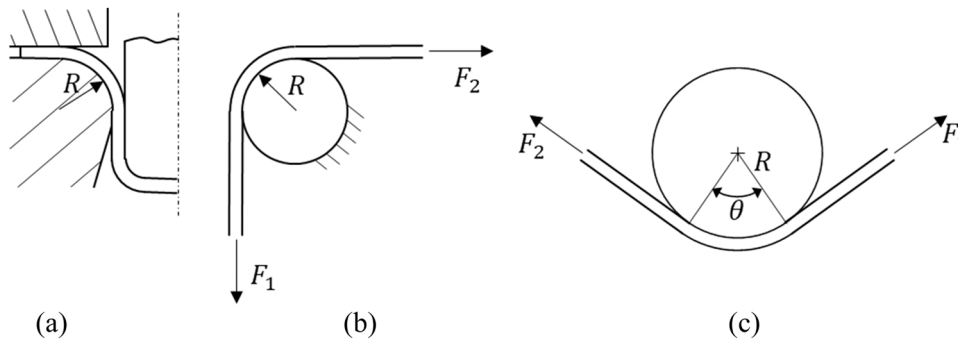


Fig. 1. Bending under tension over tool with constant radius in a) deep drawing, b) plane bending under tension adapted from [2], and c) the experimental setup of plane bending under tension suggested by Wilson et al. [3].

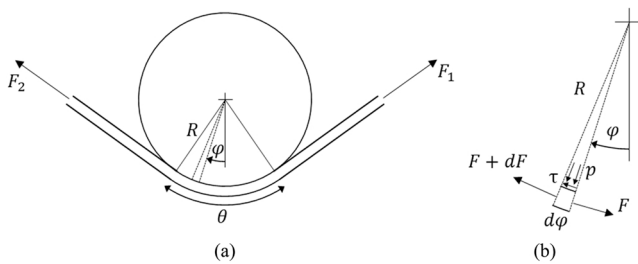


Fig. 2. Schematic used in the derivation of the belt/pulley/capstan formula by the slab method with (a) identification of a slab and (b) the slab shown in a free body diagram.

unbending of the strip from the friction estimation by carrying out two experiments. In one experiment with a freely rotating tool pin they diminished the influence from friction and found the necessary force F_b for bending and unbending of the strip. In the second experiment, the tool pin was fixed, and F_b could then be subtracted from the measured force F_1 to exclude the contribution of bending and unbending. Integration of (4) from F_2 to $F_1 - F_b$ leads to

$$\mu_{90} = \frac{2}{\pi} \ln \frac{F_1 - F_b}{F_2} \quad (7)$$

Sulonen et al. [6], who used the same method as Doege and Witthüser to determine the friction force, developed an improved

2.2. The assumption of uniform pressure

Wilson et al. [3] derived an expression for the average friction coefficient by assuming a uniform pressure distribution and therefore a uniform friction stress distribution as shown in Fig. 3a. The normal pressure is found by vertical force equilibrium,

$$(F_1 + F_2) \sin \frac{\theta}{2} = \int_{-\frac{\theta}{2}}^{\frac{\theta}{2}} p R w \cos \varphi d\varphi = 2p R w \sin \frac{\theta}{2} \quad (9)$$

$$\Leftrightarrow p = \frac{F_1 + F_2}{2Rw} \quad (10)$$

and the friction stress is found by moment equilibrium,

$$(F_1 - F_2)R = \tau w R^2 \theta \quad (11)$$

$$\Leftrightarrow \tau = \frac{F_1 - F_2}{wR\theta} \quad (12)$$

Combining (10) and (12) gives the following average coefficient of friction based on the analysis by Wilson et al. [3],

$$\Leftrightarrow \mu = \frac{\tau}{p} = \frac{2(F_1 - F_2)}{\theta(F_1 + F_2)} \quad (13)$$

In a later paper, Saha and Wilson [7] allowed the pin to rotate freely during testing, which causes a diminutive friction loss. In this way the influence of bending and unbending of the strip on the force F_1 can be

taken into account in a similar way as in (7). If F_b is subtracted from F_1 when balancing out the frictional contribution in (11), the expression for the friction coefficient becomes

$$\mu = \frac{2(F_1 - F_2 - F_b)}{\theta(F_1 + F_2)} \quad (14)$$

and in the special case of a 90° bend, the friction coefficient becomes

$$\mu_{90} = \frac{4(F_1 - F_2 - F_b)}{\pi(F_1 + F_2)} \quad (15)$$

The expressions in (14) and (15) have been widely referenced and applied, see e.g. Folle and Schaeffer [8] and Fratini et al. [9], who also attempted the derivation. They do, however, suffer from the assumption of uniform pressure being inconsistent with a constant bending moment required for the constant curvature of the strip in the tool contact, and as shown later, the system is not in equilibrium.

2.3. The assumption of uniform pressure – with torque measurement

In addition to the forces F_1 and F_2 , Andreassen et al. [10] introduced the possibility of measuring the torque induced on the tool pin by the strip. The circular cylindrical pin tool was placed in a freely rotating cradle, which was embedded in needle bearings and mounted on a torque transducer thereby enabling direct measurement of the frictional (or friction induced) torque T , see Fig. 3b. It was introduced to detect onset of galling since this is very sensitive to friction. Under the assumption of uniform pressure and friction stress, the normal pressure is known from (10), while the friction stress from a moment equilibrium is related to the measured torque through

$$\tau = \frac{T}{\theta w R^2} \quad (16)$$

From (10) and (16), the average friction coefficient equals

$$\mu = \frac{\tau}{p} = \frac{2}{\theta} \frac{T}{R(F_1 + F_2)} \quad (17)$$

and in the special case of a 90° bend, the friction coefficient becomes

$$\mu_{90} = \frac{4}{\pi} \frac{T}{R(F_1 + F_2)} \quad (18)$$

The expression in (18) has been used by e.g. Luiz and Rodrigues [11]. It suffers from the same lack of equilibrium as mentioned for the Eqs. (13)–(15).

3. Correction of the analytical solution

3.1. The lack of equilibrium with the assumption of uniform pressure

The assumptions of uniform pressure and friction stress lead to a situation that is not statically admissible, since it cannot be in equilibrium in all directions simultaneously. Horizontal force equilibrium in Fig. 3a gives

$$(F_1 - F_2)\cos\frac{\theta}{2} = \int_{-\frac{\theta}{2}}^{\frac{\theta}{2}} \tau R w \cos\varphi d\varphi = 2\tau R w \sin\frac{\theta}{2} \quad (19)$$

$$\Leftrightarrow \tau = \frac{F_1 - F_2}{2Rw} \cot\frac{\theta}{2} \quad (20)$$

This expression for the friction stress is different from that determined by moment equilibrium in (12) as often used in literature, and hence, moment and horizontal force equilibria cannot be obeyed at the same time. A similar conclusion can be drawn for the solution in (16).

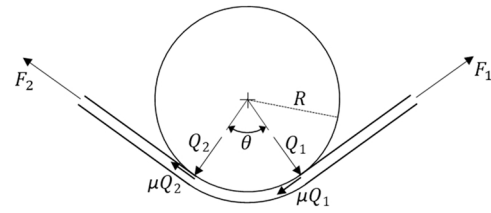


Fig. 4. Bending under tension with concentrated reaction forces on the strip.

3.2. Correction of the analytical solution

An alternative assumption of the contact conditions between the tool pin and the strip is shown in Fig. 4. The assumption of uniform pressure is here replaced by two concentrated forces, Q_1 and Q_2 , which give rise to a constant bending moment compatible with the constant curvature of the circular tool pin. This is analogous to the popular four point bending test known for its constant bending moment. The moment, horizontal force and vertical force equilibrium equations are stated in the following, where it is seen that they can all be obeyed simultaneously.

Moment equilibrium around the center of the tool pin:

$$F_1 - F_2 - \mu(Q_1 + Q_2) = 0 \quad (21)$$

Horizontal force equilibrium:

$$(F_1 - F_2)\cos\frac{\theta}{2} + (Q_1 - Q_2)\sin\frac{\theta}{2} - \mu(Q_1 + Q_2)\cos\frac{\theta}{2} = 0 \quad (22)$$

$$\Leftrightarrow (F_1 - F_2) + (Q_1 - Q_2)\tan\frac{\theta}{2} - \mu(Q_1 + Q_2) = 0 \quad (23)$$

Vertical force equilibrium:

$$(F_1 + F_2)\sin\frac{\theta}{2} - (Q_1 + Q_2)\cos\frac{\theta}{2} - \mu(Q_1 - Q_2)\sin\frac{\theta}{2} = 0 \quad (24)$$

$$\Leftrightarrow (F_1 + F_2)\tan\frac{\theta}{2} - Q_1 - Q_2 - \mu(Q_1 - Q_2)\tan\frac{\theta}{2} = 0 \quad (25)$$

From (21) and (23) it is seen that moment equilibrium and horizontal equilibrium can only co-exist if $Q_1 = Q_2$, which reduces both of the equations to

$$F_1 - F_2 - 2\mu Q_1 = 0 \quad (26)$$

while the vertical equilibrium in (25) reduces to

$$(F_1 + F_2)\tan\frac{\theta}{2} - 2Q_1 = 0 \quad (27)$$

Combining (26) and (27) results in the following friction coefficient

$$\mu = \frac{F_1 - F_2}{F_1 + F_2} \cot\frac{\theta}{2} \quad (28)$$

Also in this case, the force stemming from bending and unbending can be taken into account,

$$\mu = \frac{F_1 - F_2 - F_b}{F_1 + F_2} \cot\frac{\theta}{2} \quad (29)$$

and the special case of a 90° bend may be written as

$$\mu_{90} = \frac{F_1 - F_2 - F_b}{F_1 + F_2} \quad (30)$$

3.3. Correction of the analytical solution – with torque measurement

The friction stress in (16) was also based on the assumption of a uniform pressure distribution, which has been proven statically inadmissible. Therefore, a correction to the friction stress based on torque

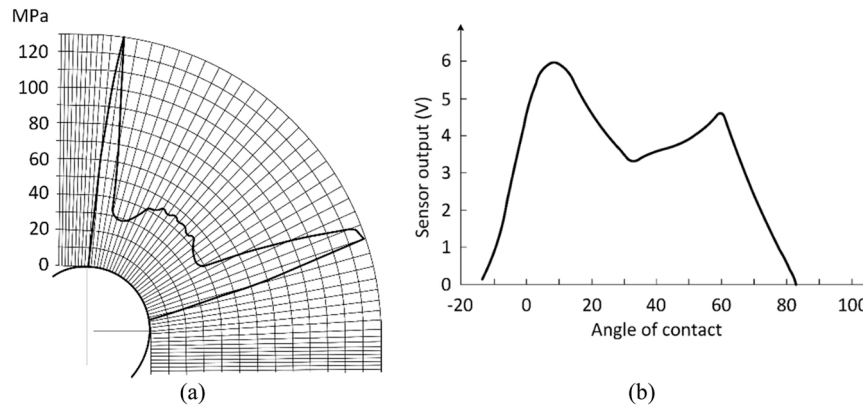


Fig. 5. Distribution of normal pressure in bending under tension determined by (a) finite element analysis with a strip drawn clockwise, and (b) experiments using a piezoelectric film with a strip drawn in the direction of increasing angle of contact. (a) Adapted from [12] (b) Adapted from [21].

measurement is also necessary. With reference to Fig. 4, and with the two concentrated forces being of same magnitude, $Q_1 = Q_2$, as found in Section 3.2, the torque equilibrium yields

$$T = \mu(Q_1 + Q_2)R = 2\mu Q_1 R \Rightarrow 2Q_1 = \frac{T}{\mu R} \quad (31)$$

Vertical force equilibrium is already formulated in (27), which in combination with (31) results in the following friction coefficient

$$\mu = \frac{T}{R(F_1 + F_2)} \cot \frac{\theta}{2} \quad (32)$$

and in the special case of a 90° bend

$$\mu_{90} = \frac{T}{R(F_1 + F_2)} \quad (33)$$

which differ from (18) by a factor $\pi/4$.

3.4. Comparison with existing numerical solutions

Several studies in literature have discussed the fact that the normal pressure is not uniformly distributed, but instead has a profile with peaks near the ends of the contact arc. This supports the assumption of concentrated forces in the analytical solution based on Fig. 4. Both simulations and measurements have been applied to identify the pressure distribution in bending under tension.

Sniekers and Smits [12] applied finite element analysis to determine the pressure distribution in the tool-workpiece interface in bending under tension testing of a 1 mm mild C-steel strip drawn over a $\varnothing 10$ mm pin tool. Their result is reproduced in Fig. 5a, where it is noticed that the pressure distribution is highly inhomogeneous, and two pressure peaks appear at approximately 6° after the inlet and 15° before the outlet. These peaks are due to the bending moment at the inlet and unbending moment at the outlet of the contact interface. Similar numerical results have been presented by Pereira et al. [13] and by a number of researchers who also noticed the wear developing at these two locations, see e.g. Mortensen et al. [14], Hörtig and Schmoekel [15], Pereira et al. [16], Groche et al. [17], and Ceron and Bay [18]. The three dimensional pressure distribution has been simulated by Ersoy-Nürnberg et al. [19] and Kim et al. [20].

Coubrough et al. [21] determined the pressure distribution in bending under tension experimentally by using a specially processed polyvinylidene fluoride (PVDF) polymer, known as Kynar® piezoelectric sensor. On a freely rotating $\varnothing 12.7$ mm pin tool the sensor was able to move together with the strip as this was pulled around the pin tool. Fig. 5b shows the measured sensor output in volts along the contact zone in a 90° bending under tension test of 0.74 mm thick low C-steel. The

sensor output is proportional to the pressure distribution with peak values in the entry and exit zone similar to the one determined by the above mentioned finite element simulations.

4. Conclusion

The previous analytical solutions based on the assumption of a uniform pressure in the contact between tool and workpiece in the bending under tension test suffer from statically inadmissible conditions, since horizontal force and moment equilibriums cannot co-exist. An alternative assumption based on concentrated forces at the ends of the contact zone has been suggested, and the corresponding analytical expressions have been derived while showing moment, horizontal force and vertical force equilibrium. Both numerical solutions and experimental results in literature support the proposed assumption for the analytical solution. Given the highly inhomogeneous pressure distribution, determination of a mean coefficient of friction $\mu = \tau/p$, where τ is the average friction stress and p is the average normal pressure in the nominal contact zone is of little practical use. The bending under tension test should be used only as a relative comparison of friction coefficients or in investigations of lubricant breakdown and onset of galling when comparing the quality of different lubricants or other parameters in tribo-systems.

Declaration of Competing Interest

The authors declare that they have no known competing financial interests or personal relationships that could have appeared to influence the work reported in this paper.

Acknowledgements

This research was partly funded by Independent Research Fund Denmark, grant number DFF -0136-00159.

References

- [1] Swift HW. Plastic bending under tension. *Engineering* 1948;3:333-59.
- [2] Littlewood M, Wallace JF. Effect of surface finish and lubrication on frictional variations involved in sheet-metal-forming process. *Sheet Met Ind* 1964;41(452): 925-30.
- [3] Wilson WRD, Malkani HG, Saha PK. Boundary friction measurements using a new sheet metal forming simulator. *Transactions of NAMRI/SME*. 1991. p. 37-42.
- [4] Higdon A, Stiles WB. *Engineering Mechanics*. New York: Prentice Hall Inc; 1955.
- [5] Doege E, Witthüser KP. HfH-Bericht 9. UKH. Hannover: Gesellschaft für Produktionstechnik; 1977.
- [6] Sulonen M, Eskola P, Kumpulainen J, Ranta-Eskola A. (1981) A reliable method for measuring the friction coefficient in sheet metal forming. In: IDDRG Working Group Meeting. WG3/5/81, 1-15.
- [7] Saha PK, Wilson WRD. Influence of plastic strain on friction in sheet metal forming. *Wear* 1994;172:167-73.

- [8] Folle L, Schaeffer L. New proposal to calculate the friction in sheet metal forming through bending under tension test. *Mater Res* 2019;22(6):e20190523.
- [9] Fratini L, Casto SL, Valvo EL. *J Mater Process Technol* 2006;172:16–21.
- [10] Andreassen JL, Olsson DD, Chodnikiewicz K, Bay N. Bending under tension test with direct friction measurement. *Proc Inst Mech Eng, Part B: J Eng Manuf* 2006;220(1):73–80.
- [11] Luiz VD, Rodrigues PCM. Design of a tribo-simulator for investigation of the tribological behavior of stainless-steel sheets under different contact conditions. *Mater Res* 2022;25:e20210220.
- [12] Sniekers RJJM, Smits HAA. Experimental set-up and data processing of the radial strip-drawing friction test. *J Mater Process Technol* 1997;66(1–3):216–23.
- [13] Pereira MP, Duncan JL, Yan W, Rolfe BF. Contact pressure evolution at the die radius in sheet metal stamping. *J Mater Process Technol* 2009;209:3532–41.
- [14] Mortensen J., Dirks J., Christensen P. (1994) A combined physical and numerical simulation of tool performance in conventional deep-drawing operations. In: *Proceedings of the International Deep-Drawing Research Group, 18th Biennial Congress, 233–240.*
- [15] Hortig D, Schmoedel D. Analysis of local loads on the draw die profile with regard to wear using the FEM and experimental investigations. *J Mater Process Technol* 2001;115:153–8.
- [16] Pereira MP, Yan W, Rolfe BF. Contact pressure evolution and its relation to wear in sheet metal forming. *Wear* 2008;265:1687–99.
- [17] Groche P, Nitzsche G, Elsen A. Adhesive wear in deep drawing of aluminum sheets. *CIRP Ann - Manuf Technol* 2008;57:295–8.
- [18] Ceron E, Bay N. Determination of friction in sheet metal forming by means of simulative tribo-tests. *Key Eng Mater* 2013;549:415–22.
- [19] Ersoy-Nürnberg K, Nürnberg G, Golle M, Hoffmann H. Simulation of wear on sheet metal forming tools — an energy approach. *Wear* 2008;265:1801–7.
- [20] Kim YS, Jain MK, Metzger DR. Determination of pressure-dependent friction coefficient from draw-bend test and its application to cup drawing. *Int J Mach Tools Manuf* 2012;56:69–78.
- [21] Coubrough GJ, Allinger MJ, Van Tyne CJ. Angle of contact between sheet and die during stretch-bend deformation as determined on the bending-under-tension friction test system. *J Mater Process Technol* 2002;130–131:69–75.